Ref. Ares(2020)7201726 - 30/11/2020

# Deliverable 7.2: Scientific Characterization


**Authors** Loris Colombo
Hans Kristian Eriksen
Simone Paradiso


**Date** November 25th, 2020

**Work Package** WP7 - Physical Interpretation

# Revision History

| | | | |
|---|---|---|---|
| Version | Authors | Date | Changes |
| 1.0 | Loris Colombo<br>Hans Kristian Eriksen<br>Simone Paradiso | November 25th, 2020 | Initial Version |

# Contents

# 1. Introduction

The BeyondPlanck project lead to a huge array of results including, among others: new computational frameworks, improved characterization of Planck LFI instrument, and new maps of astrophysical components. From a cosmological point of view, the main results are the new maps of Cosmic Microwave Background (CMB) and the resulting constraints on cosmological parameters.

More in details, three sets of CMB maps were produced by BeyondPlanck, optimized for different scientific goals:

- **Component separation targeted maps.** Within the primary Gibbs chain, we solve for CMB temperature and polarization fluctuation amplitudes together with the amplitudes of the other diffuse components (e.g. thermal dust, synchrotron radiation), applying neither an isotropy prior on the CMB components, nor a processing mask. This choice is computationally the fastest, at the penalty of slightly suboptimal maps: CMB maps are less smooth than with a spatial prior, and astrophysical emission residuals are visible in the Galactic plane. The main goal of this step of the pipeline is the production of robust foregrounds estimates, which in turn lead to better gain estimation and cleaner frequency maps. For this purpose, the features of CMB maps described above are not a limitation. On the other hand, for the final cosmological analysis we produce additional CMB maps free from the above limitation by post processing the primary chain samples.
- **Full resolution cosmological analysis temperature maps.** For each primary chain sample, we generate a new CMB map fixing the non-CMB parameters to the value they had at that step of the primary chain, but applying a processing mask and an isotropy prior. In this run, we also sample the CMB power spectrum at each chain step. With this setup, solving for the CMB map is more computationally expensive than in the primary chain, but the resulting CMB maps are noiseless and fullsky (the area within the processing mask is filled with a constrained realization), and power spectrum sampling is straightforward. These maps and power spectra form the basis for the Gaussianized Blackwell-Rao likelihood used for estimating cosmological parameters at intermediate and small angular scales.
- **Low resolution cosmological analysis maps.** Given Planck LFI properties, polarization measurements on scales smaller than ~20º are completely noise dominated and do not provide significant cosmological information. Even at larger scales, the signal-to-noise ratio is modest, and a proper likelihood analysis needs an accurate description of the instrumental noise and residual systematics effects. This contrasts with temperature analysis, where all scales we include in the likelihood are strongly signal dominated. Taking these facts into account, for the analysis of large angular scales we work directly at low resolution. For each primary chain sample, we fix the non-CMB parameters and the CMB multipoles larger than $\ell = 64$ (corresponding to ~ 3º) and generate 50 low-resolution temperature and polarization maps, assuming no isotropy prior and no processing mask. After post-processing the full primary chain, we have a distribution of 45000 low resolution samples that we use to compute the posterior mean map and corresponding effective

noise covariance, which form the basis of the compressed Gaussian likelihood used for estimating cosmological parameters at large angular scales.

One important aspect of both reprocessing steps is that, while each individual resampled map corresponds to specific values of instrumental and foregrounds parameters, by repeating the resampling for all primary chain steps we are effectively marginalizing over such parameters.

# 2. CMB maps

Both sets of resampled maps, and the corresponding likelihood datasets, are available through the BeyondPlanck website (https://beyondplanck.science/products/files/), and described in detail in the collaboration papers (BeyondPlanck Collaboration 2020, Colombo et al. 2020, Paradiso et al. 2020). As the primary chain CMB maps are only used internally and not for the final cosmological results, we decided to not release them separately, to minimize possible confusion to external users. As the full pipeline and corresponding input files are publicly available, interested users have anyway the possibility to recreate those maps on their own.

## 2.1 Full resolution T maps

Each resampled map represents a realization of a fullsky noiseless CMB field, compatible with the observed microwave sky. Therefore, analysis of these samples is particularly straightforward, as it does not require noise modeling or masking. On the other hand, the posterior mean corresponds to a Wiener-filtered map, and is thus a biased estimate of the CMB sky, with angular scales affected by larger noise being suppressed more than scales with lower noise. In addition, the area inside the processing mask is filled with a constrained realization.

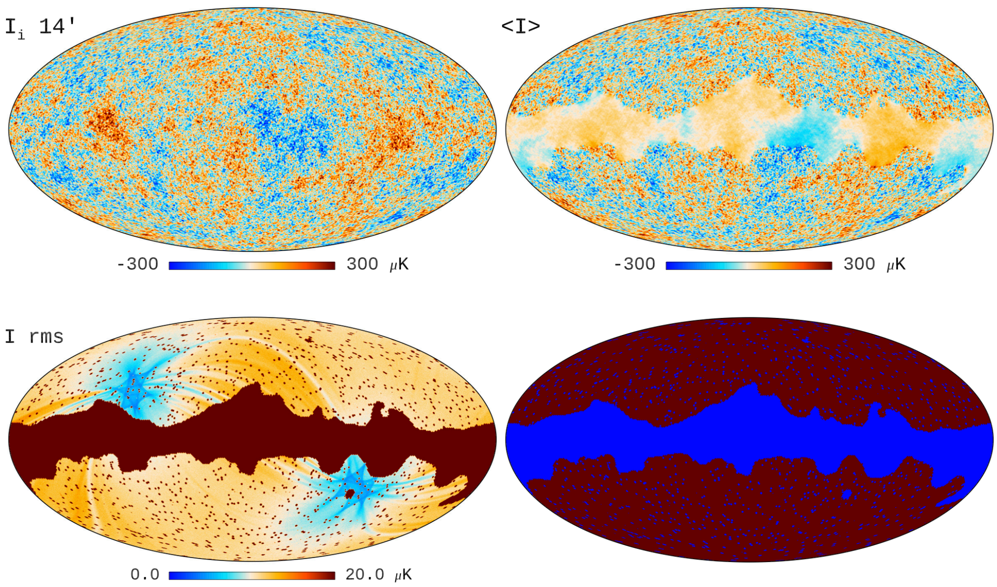


Figure 1. Clockwise from top left: Single sample, Posterior mean, Processing mask, Standard deviation.

While individual samples represents noiseless fullsky CMB maps, the overall distribution encodes information on noise, instrumental and foregrounds parameters explored by the primary chain. A clear representation of this is provided by the samples standard deviation, which shows the imprint of Planck scanning strategy outside the processing mask, while inside the mask the standard deviation is dominated by the random phases of the constrained realizations.

This feature of BeyondPlanck results requires a shift in the way CMB products are analyzed. In traditional CMB data analysis, a single CMB map or power spectrum were produced, corresponding to the best-fit solution under specific assumptions for instrumental parameters, and were used as input for the likelihood analysis. Uncertainty estimates were based on forward simulations and/or splitting the data into different subsets (e.g. surveys, detectors).

BeyondPlanck samples, instead, provide a straightforward and self-consistent way to propagate uncertainties on the final science results, by applying the estimator of interest to each of the samples and then computing means, standard deviations, higher moments, etc. from the resulting distribution. An example of this strategy is provided by the CMB power spectrum itself. Within the post-processed chain, we draw a power spectrum sample from each resampled map. The resulting mean power spectrum is shown in Fig. 2, while the full distribution is used in the Gaussianized Blackwell-Rao likelihood for cosmological parameter estimation (Paradiso et al. 2020).

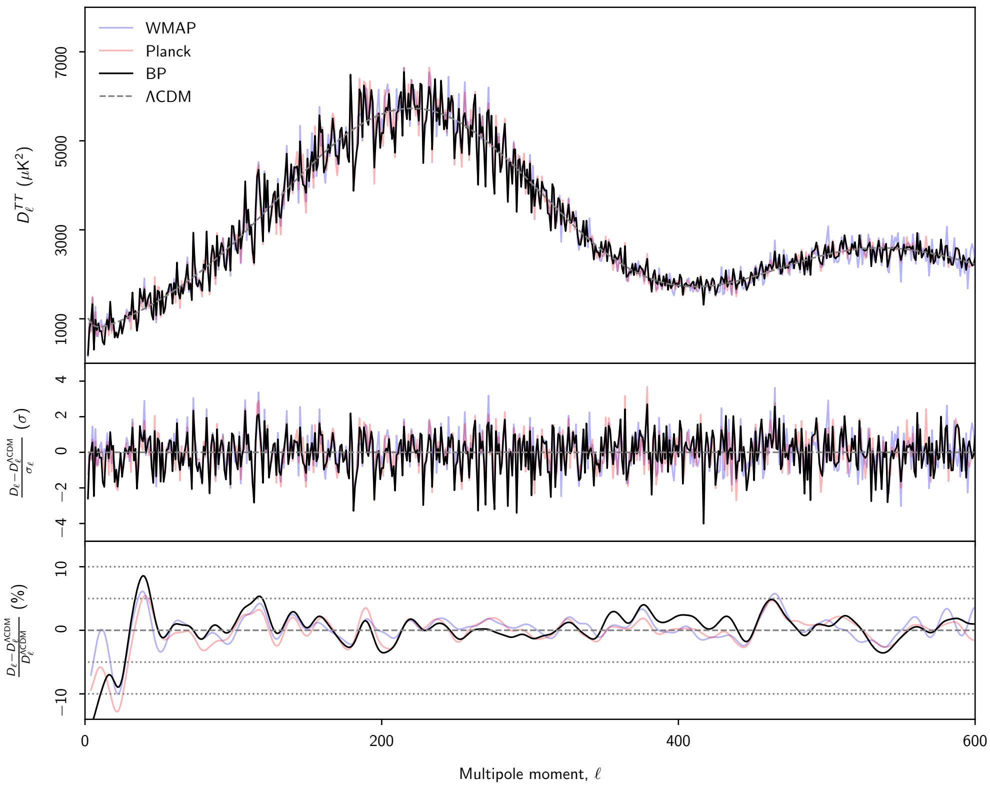


Figure 2. Top: CMB power spectrum for WMAP, Planck 2018, and BeyondPlanck compared to the ΛCDM bestfit model. Middle: Difference between estimated power spectrum and ΛCDM bestfit model in unit of the uncertainty quoted by the respective pipelines. Bottom: Fractional difference with respect to ΛCDM bestfit

## 2.2 Low resolution maps

Fig.3 shows the low-resolution Stokes Q and U posterior mean. Since we do not apply an isotropy prior and a processing mask, Galactic emission residuals are visible in the plane, and we therefore exclude this portion of the sky from the final likelihood analysis. In addition, goodness of fit tests failed when including the Southern hemisphere. Such failures were traced to unmodelled excess noise in 30 and 44GHz maps, and gain-correlated stripes at 44GHz, and we conservatively decided to also exclude the Southern hemisphere, leaving ~ 36% of the sky for the cosmological parameter estimation.

This approach was motivated from the need to provide an accurate noise modeling, in terms of an effective noise covariance matrix (NCVM), to avoid biasing the science analysis. In traditional CMB pipelines, the final CMB map corresponds to a specific set of instrumental and noise parameters, for whom a NCVM can be computed from first principles. For BeyondPlanck each sample corresponds to different instrumental parameters and would in principle require a different NCVM. Since NCVM computation is very expensive, this is clearly unfeasible. We thus adopted the alternative approach of computing the effective NCVM directly from the samples, which has the added benefit of incorporating other systematics (e.g. component separation residuals) without any additional modeling. Even at low resolution, brute force estimation of the NCVM requires several tens of thousands of samples for stable results. In order to optimize the computational time, we further compress the CMB map by projecting out modes with low signal-to-noise. While the likelihood for the compressed map has the same functional form as the one for the uncompressed map (specifically, a multivariate Gaussian distribution), the compression procedure allows to significantly reduce the number of samples required for a robust NCVM.

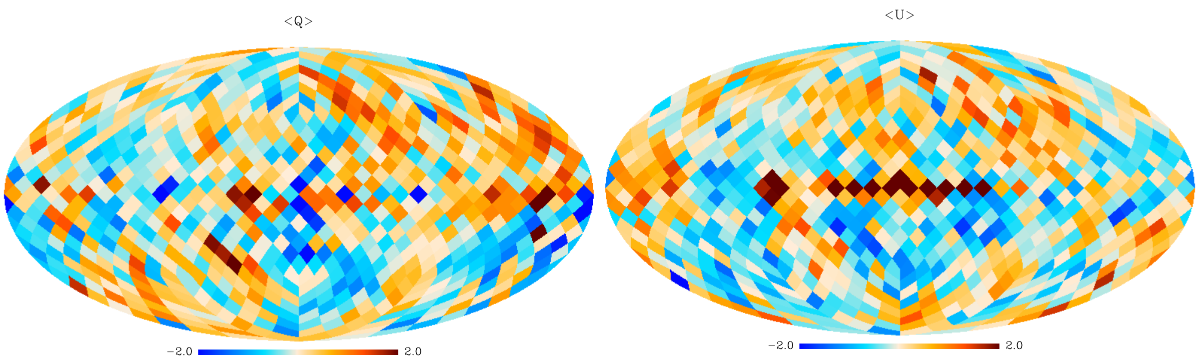


Figure 3. Posterior mean low resolution Stokes Q and U resampled CMB maps.

# 3. Cosmological parameters

The main Planck 2018 cosmological parameter constraints are based on HFI data, which have superior sensitivity and resolution compared to LFI data. Therefore, while BeyondPlanck constraints are in good agreement with current estimates, at face value they are not competitive in terms of error bars. However, even discounting the differences between HFI and LFI performances, we would expect BeyondPlanck constraints to display larger uncertainties than corresponding traditional pipelines, due to the marginalization over instrumental and foreground uncertainties. This is well exemplified by Fig. 4, which shows how the posterior distribution for the Optical Depth to Reionization from BeyondPlanck low-$\ell$ likelihood becomes larger as we marginalize over a wider set of non-CMB parameters.

In principle, a similar effect would also impact constraints based on BeyondPlanck full resolution temperature data, but at the angular scales we included in our analysis noise and systematics are well below CMB signal, and the increase in error bars is minimal. Nevertheless, these results represent the first time in which instrumental and foregrounds sources of uncertainties have been fully and self-consistently propagated to the final cosmological constraints. We show such constraints, and a comparison with results from Planck 2018 and WMAP in Table 5.

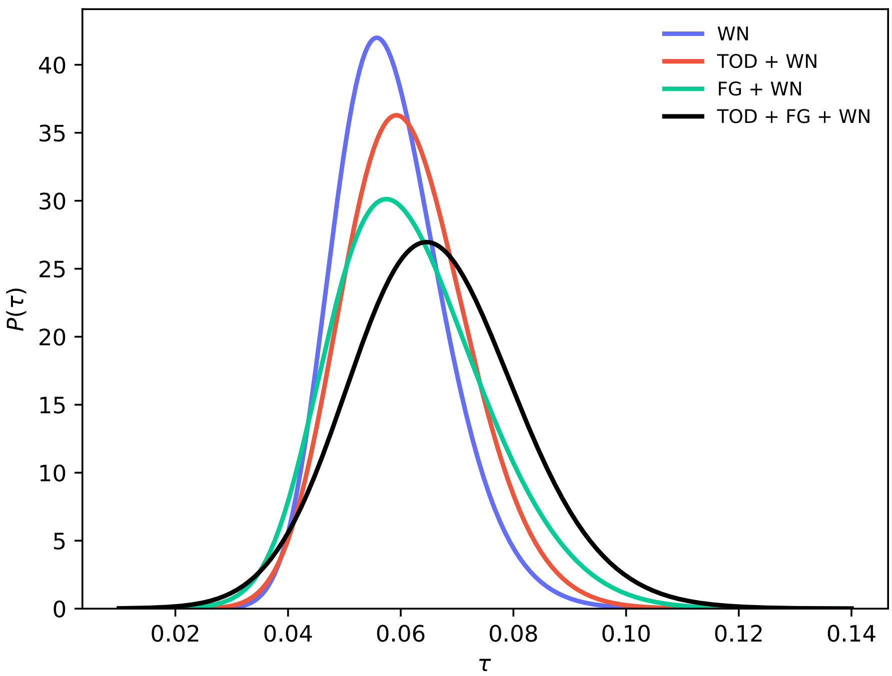


Figure 4. Posterior probability distribution for the Optical Depth to Reionization, τ, based on BeyondPlanck low-$\ell$ data. Different curves correspond to marginalization over different sets of non-CMB parameters: white noise (WN), Galactic astrophysical emission (FG), gain, correlated noise and instrumental effects (TOD).

**Table 5.** Comparison of basic 6-parameter ΛCDM model parameters as derived by BeyondPlanck (Paradiso et al. 2020), *Planck* 2018 (Planck Collaboration VI 2020), and *WMAP* (Hinshaw et al. 2013). The second column shows results for BeyondPlanck only, using only $TT$ multipoles below $\ell \leq 600$ and polarization below $\ell \leq 8$. The third column shows similar results when also adding $TT$ multipoles between $600 < \ell \leq 2500$ from *Planck* 2018. For *Planck*, we show results from the `Plik` pipeline using the $TT$+$TE$+$EE$+lowE+lensing data combination, while for *WMAP* we show results based on $C^{-1}$-weighted 9-year *WMAP*-only data. Note that *Planck* and *WMAP* adopt slightly different conventions for some parameters, and we report both where applicable. Columns marked with "Δ" show differences with respect to BeyondPlanck-only results, as measured in units of $\sigma$.

| | BeyondPlanck | | *Planck* 2018 | | *WMAP* | |
|---|---|---|---|---|---|---|
| Parameter | $\ell \leq 600$ | +*Planck* $\ell > 600$ | Estimate | $\Delta\,(\sigma)$ | Estimate | $\Delta\,(\sigma)$ |
| $\Omega_b h^2$ | $0.02226 \pm 0.00088$ | $0.02230 \pm 0.00022$ | $0.02237 \pm 0.00015$ | −0.1 | $0.02243 \pm 0.00050$ | −0.2 |
| $\Omega_c h^2$ | $0.115 \pm 0.016$ | $0.1227 \pm 0.0025$ | $0.1200 \pm 0.0012$ | −0.3 | $0.1147 \pm 0.0051$ | 0 |
| $\Omega_\Lambda$ | ... | ... | ... | ... | $0.721 \pm 0.025$ | ... |
| $100\theta_{MC}$ | $1.0402 \pm 0.0048$ | $1.04064 \pm 0.00048$ | $1.04092 \pm 0.00031$ | −0.2 | ... | ... |
| $\tau$ | $0.067 \pm 0.016$ | $0.074 \pm 0.015$ | $0.054 \pm 0.007$ | 0.8 | $0.089 \pm 0.0014$ | −1.4 |
| $10^9 \Delta^2_{\mathcal{R}}$ | ... | ... | ... | ... | $2.41 \pm 0.10$ | ... |
| $\ln(10^{10} A_s)$ | $3.035 \pm 0.079$ | $3.087 \pm 0.029$ | $3.044 \pm 0.014$ | −0.1 | ... | ... |
| $n_s$ | $0.962 \pm 0.019$ | $0.9632 \pm 0.0060$ | $0.9649 \pm 0.0042$ | −0.1 | $0.972 \pm 0.013$ | −0.5 |

# 4. References

[1] BeyondPlanck Collaboration (2020), *BeyondPlanck I. Global Bayesian analysis of the Planck Low Frequency Instrument data.* A&A submitted, https://arxiv.org/abs/2011.05609.

[2] Colombo et al. (2020), *BeyondPlanck XI. CMB analysis with end-to-end error propagation: Temperature anisotropies*. A&A, to be submitted.

[3] Paradiso et al. (2020), *BeyondPlanck XII. CMB analysis with end-to-end error propagation: Likelihood and Cosmological Parameters*. A&A, to be submitted.